Wind and Structures, Vol. 10, No. 3 (2007) 233-247
DOI: http://dx.doi.org/10.12989/was.2007.10.3.233

Control of the along-wind response of steel framed buildings by using viscoelastic or friction dampers

Fabio Mazza† and Alfonso Vulcano‡

Dipartimento di Strutture, Università della Calabria, 87036 Arcavacata di Rende (Cosenza), Italy

(Received September 23, 2006, Accepted April 1, 2007)

Abstract. The insertion of steel braces has become a common technique to limit the deformability of steel framed buildings subjected to wind loads. However, when this technique is inadequate to keep floor accelerations within acceptable levels of human comfort, dampers placed in series with the steel braces can be adopted. To check the effectiveness of braces equipped with viscoelastic (VEDs) or friction dampers (FRDs), a numerical investigation is carried out focusing attention on a three-bay fifteen-storey steel framed building with K-braces. More precisely, three alternative structural solutions are examined for the purpose of controlling wind-induced vibrations: the insertion of additional diagonal braces; the insertion of additional diagonal braces equipped with dampers; the insertion of both additional diagonal braces and dampers supported by the existing K-braces. Additional braces and dampers are designed according to a simplified procedure based on a proportional stiffness criterion. A dynamic analysis is carried out in the time domain using a step-by-step initial-stress-like iterative procedure. Along-wind loads are considered at each storey assuming the time histories of the wind velocity, for a return period T_r=5 years, according to an equivalent wind spectrum technique. The behaviour of the structural members, except dampers, is assumed linear elastic. A VED and an FRD are idealized by a six-element generalized model and a bilinear (rigid-plastic) model, respectively. The results show that the structure with damped additional braces can be considered, among those examined, the most effective to control vibrations due to wind, particularly the floor accelerations. Moreover, once the stiffness of the additional braces is selected, the VEDs are slightly more efficient than the FRDs, because they, unlike the FRDs, dissipate energy also for small amplitude vibrations.

Keywords: passive control; wind vibration control; energy dissipation; damped braced frames; dissipative braces; viscoelastic dampers; friction dampers; design of dissipative braces.

1. Introduction

The conventional design of steel framed buildings subjected to wind loads is pursued by using structural elements with appropriate strength and stiffness properties, such as to keep the response elastic and to prevent buckling. Moreover, in order to improve comfort for building occupants and the serviceability of the equipment, the insertion of steel braces (e.g. diagonal, cross or chevron braces) is usually adopted to limit displacements and accelerations induced at the floor levels by the wind loads. In case this technique should be insufficient, the wind response of a building can be

† Ph.D., Researcher, E-mail: fabio.mazza@unical.it
‡ Professor, Corresponding Author, E-mail: vulcano@unical.it

improved by means of recent vibration control techniques, making use of suitable mechanical systems which provide the structure with additional damping (i.e. passive-, semi-active and active-type systems), or adopting aerodynamic modifications (e.g. using sectional shapes chamfered or cut in plan and/or tapered in elevation, "ad hoc" openings, fins, etc.). For a general discussion about these techniques see the works of Housner, *et al*. (1997), Tamura (1998) and Kareem, *et al*. (1999).

Among the passive control systems, the insertion of steel braces equipped with dissipative devices ("dissipative braces") proves to be effective to reduce wind-induced vibrations. In the last few decades several applications have been realized in different countries and nowadays a wide variety of energy dissipating devices is available (Soong and Dargush 1997). Apart from special devices (e.g. shape memory alloys and electro- or magneto-rheological devices), a lot of damping devices can be broadly classified in two categories: (a) rate independent, i.e., dampers dissipating energy by friction or metallic-yielding; (b) rate-dependent, i.e., dampers based on viscoelasticity or viscosity of elastomers or fluids. To allow a widespread application of passive dampers, practical design procedures should be available aiming at an optimum proportioning in order that a designated level of wind protection is achieved. In this perspective, a comparative study is carried out in this paper checking the effectiveness of viscoelastic and friction dampers, which are supported by either the bracing system existing in the structure or an additional one.

2. Viscoelastic and friction dampers

A viscoelastic damper (VED) consists of layers of a viscoelastic (VE) polymer constrained by means of steel plates whose damping effect depends on heat loss when subjected to shearing. The behaviour of a VED is idealized as linear with regard to displacement and velocity; thus, under a sinusoidal motion of amplitude Δ_0 and circular frequency ω_D, it can be simulated by the skew elliptical force-displacement (N_D-Δ_D) law shown in Fig. 1(a), where the force (N_D) is partially out of phase with the imposed displacement (Δ_D). The characteristic parameters of a VED are the storage stiffness $K'_D(=G'A/h)$, which represents the slope of the axis simulating the elastic response contribution, and the loss stiffness $K''_D\,(=G''A/h)$, which gives a measure of the energy dissipation for cycle. These parameters depend on the mechanical properties of the VE material, i.e., the shear storage modulus (G') and the shear loss modulus (G''), as well as on the shear area (A) and the total thickness of the polymer layers (h). The observed behaviour of a VED shows an increase of G' and G'' for increasing load frequency; the opposite one occurs for an ever-higher ambient temperature (e.g. Samali and Kwok 1995, Shen and Soong 1995). Moreover, if the damper temperature increases too much, the idealization of linear VE behaviour may be unrealistic.

The behaviour of a VED can be simulated by the six-element generalized model (GM) shown in Fig. 1(b), which is an in-parallel-combination of one Kelvin model (KM) and two Maxwell models (MMs), i.e., classical linear VE models constituted of an elastic spring and a dashpot acting in parallel (KM) or in series (MM). The GM allows, unlike a single KM or MM, a better description of the variation of G' and G'' for varying values of the excitation frequency at a given ambient temperature. Indeed, a single KM or MM can be calibrated to match exactly the experimental values of G' and G'' corresponding only to a single value of the frequency at a given temperature. Further details on the calibration of all the above models can be found in a previous work by the authors (Mazza and Vulcano 2001).

In particular, using the GM in Fig. 1(b), the storage stiffness, K'_D, and the loss stiffness, K''_D, can be expressed, for a given circular frequency, ω_D, as functions of the constants characterizing the behaviour of the elastic springs (i.e. $K_{D,i}$) and the dashpots (i.e. $C_{D,i}$):

$$K'_D = \omega_D^2\left(\frac{K_{D,1}C_{D,1}^2}{\omega_D^2 C_{D,1}^2 + K_{D,1}^2} + \frac{K_{D,2}C_{D,2}^2}{\omega_D^2 C_{D,2}^2 + K_{D,2}^2}\right) + K_{D,3} \tag{1a}$$

$$K''_D = \omega_D\left(\frac{K_{D,1}^2 C_{D,1}}{\omega_D^2 C_{D,1}^2 + K_{D,1}^2} + \frac{K_{D,2}^2 C_{D,2}}{\omega_D^2 C_{D,2}^2 + K_{D,2}^2} + C_{D,3}\right) \tag{1b}$$

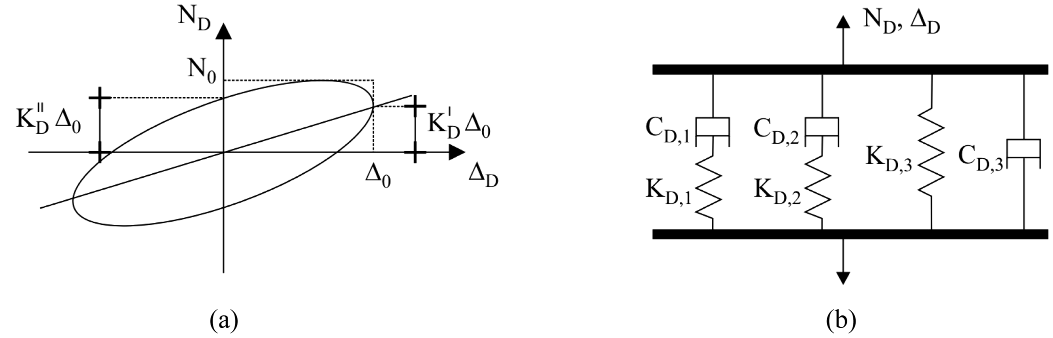

Fig. 1 Idealized response for a sinusoidal motion (a) and generalized model, GM (b), of a viscoelastic damper

A friction damper (FRD) is characterized by a sliding mechanism with stable cyclic behaviour and an energy dissipation practically independent of the load frequency and temperature; its activation happens when a preset threshold force is reached. The behaviour of an FRD can be simply idealized by a rigid-plastic force-displacement (N_D-Δ_D) law (Fig. 2a), which is simulated by the model shown in Fig. 2(b), where N_{Fr} represents the slip load. The selection of the N_{Fr} value should ensure an effective control of the wind-induced vibrations in such a way that the device does not slip under normal service gravity loads and expected wind actions of low intensity.

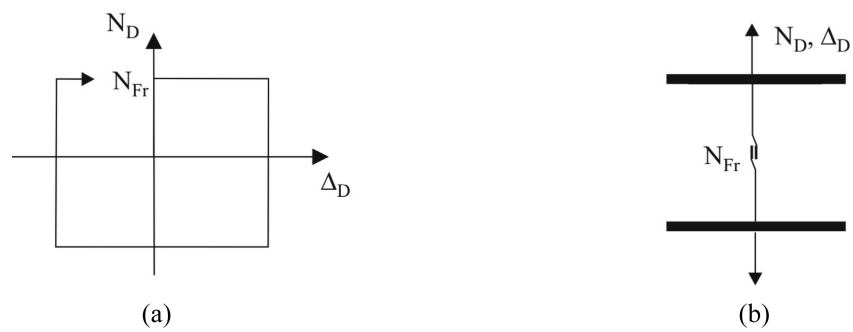

Fig. 2 Idealized response (a) and modelling (b) of a friction damper

3. Design of the test structure and vibration control systems

For the sake of clarity, a three-bay fifteen-storey steel building, whose symmetric plan is shown in

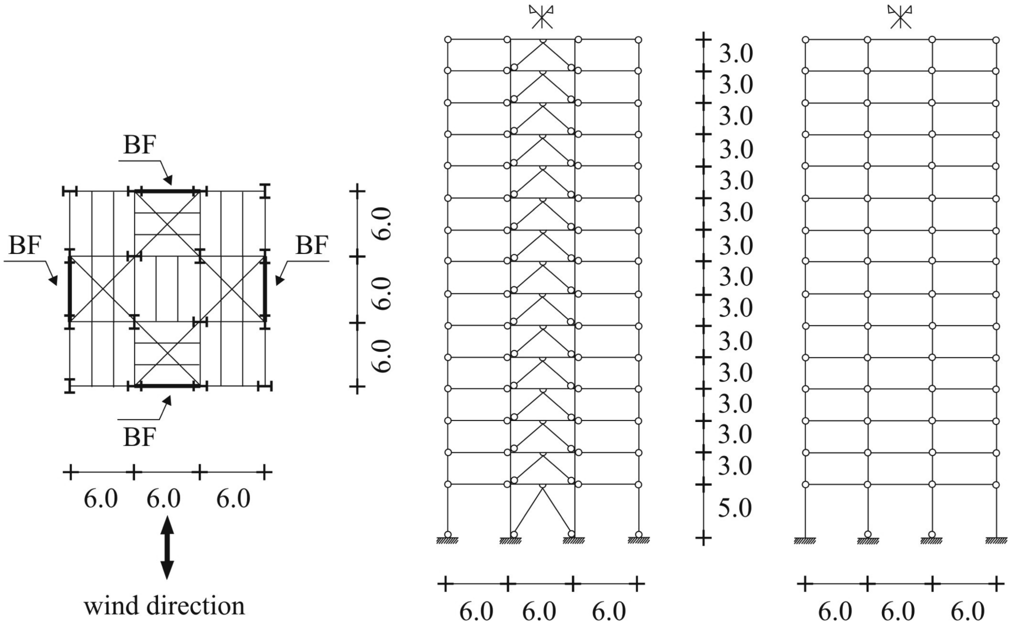

(a) Plan (b) A perimeter frame (BF) (c) An interior frame

Fig. 3 Test structure (dimensions in metres)

Fig. 3(a), is considered as a test structure for the numerical investigation. More precisely, four perimeter frames with concentric K-braces placed in the central bay (a perimeter Braced Frame, BF, is shown in Fig. 3b) are capable of carrying horizontal (wind) as well as gravity loads, while four interior frames (Fig. 3c), likewise the lateral bays of each BF, are made up of pin-ended strut-and-tie members which contribute to support only the vertical loads.

The test structure (without dissipative devices), subjected to gravity and wind loads, is designed in accordance with the provisions of Eurocode 3 (EC3 2003). Specifically, high deformability and buckling are prevented checking, respectively, the serviceability limit and ultimate state. The gravity loads at the top floor or other floors are assumed to be constituted of dead loads of 3.17 or 4.11 kN/m^2, respectively, and by live loads of 0.75 or 3.00 kN/m^2, respectively. The weight of sandwich panels, regularly distributed in elevation as external cladding of the building, is taken into account considering a dead load of 0.4 kN/m^2.

Wind actions for the Italian climate are evaluated complying with Eurocode 1 (EC1 2004), assuming: flat terrain with a roughness length of 0.30 m; urban area (class B of terrain roughness) with a reference velocity of 28 m/s, which represents a mean value of those assumed for the nine zones of the Italian wind map; an altitude of 600 m above sea level.

The member cross-sections of a perimeter BF and those of an interior frame, designed assuming EC3 class sections 1 or 2 and a steel ultimate strength of 510 N/mm^2, are reported in Table 1 and Table 2, respectively. In Table 1 is also reported the (elastic) lateral stiffness distribution of a BF (i.e. the ratio $K_{BF,i}/K_{BF,1}$, being: $K_{BF,i}$=lateral stiffness of a generic storey; $K_{BF,1}$=lateral stiffness of the first storey=1.646x10^5 kN/m). The fundamental vibration period of the test structure is 2.564 s.

For the purpose of controlling the wind-induced vibrations of the test structure in Fig. 3, the

Table 1 Member cross-sections and distribution of the lateral stiffness ($K_{BF,i}$) for a perimeter braced frame (BF)

	Girders		Columns		K-braces	
Storey	Exterior	Interior	Exterior	Interior	Central bay	$K_{BF,i}/K_{BF,1}$ (*)
15	IPE 270	IPE 270	HEB 180	HEB 200	2L 100x10	0.015
14	IPE 270	IPE 300	HEB 180	HEB 200	2L 100x10	0.042
13	IPE 270	IPE 300	HEB 180	HEB 200	2L 100x10	0.068
12	IPE 270	IPE 300	HEB 180	HEB 200	2L 100x10	0.094
11	IPE 270	IPE 330	HEB 180	HEB 200	2L 100x10	0.122
10	IPE 270	IPE 330	HEB 200	HEB 220	2L 100x10	0.152
9	IPE 270	IPE 330	HEB 200	HEB 240	2L 100x16	0.194
8	IPE 270	IPE 360	HEB 200	HEB 280	2L 100x16	0.234
7	IPE 270	IPE 360	HEB 200	HEB 300	2L 100x16	0.278
6	IPE 270	IPE 360	HEB 220	HEB 320	2L 120x13	0.337
5	IPE 270	IPE 360	HEB 220	HEB 360	2L 120x13	0.404
4	IPE 270	IPE 400	HEB 220	HEB 400	2L 120x13	0.510
3	IPE 270	IPE 400	HEB 240	HEB 450	2L 120x13	0.650
2	IPE 270	IPE 400	HEB 240	HEB 500	2L 120x13	0.889
1	IPE 270	IPE 400	HEB 260	HEM 600	2L 150x18	1.000

(*) $K_{BF,1}$=1.646x10^5 kN/m

Table 2 Member cross-sections for an interior frame

	Girders		Columns	
Storey	Exterior	Interior	Exterior	Interior
15	IPE 270	IPE 270	HEB 200	HEB 200
14	IPE 330	IPE 330	HEB 200	HEB 200
13	IPE 330	IPE 330	HEB 200	HEB 200
12	IPE 330	IPE 330	HEB 200	HEB 200
11	IPE 330	IPE 330	HEB 200	HEB 220
10	IPE 330	IPE 330	HEB 220	HEB 260
9	IPE 330	IPE 330	HEB 240	HEB 280
8	IPE 330	IPE 330	HEB 280	HEB 300
7	IPE 330	IPE 330	HEB 300	HEB 320
6	IPE 330	IPE 330	HEB 320	HEB 340
5	IPE 330	IPE 330	HEB 360	HEB 400
4	IPE 330	IPE 330	HEB 400	HEB 400
3	IPE 330	IPE 330	HEB 450	HEB 450
2	IPE 330	IPE 330	HEB 500	HEB 500
1	IPE 330	IPE 330	HEM 600	HEB 550

addition of diagonal braces in the lateral bays of each perimeter BF is basically considered. Then, three alternative structural solutions are examined with reference to the insertion of dampers inside a perimeter BF: no dampers (AB: “Additional Braces”; Fig. 4a); the insertion of dampers supported by the additional diagonal braces (DAB: “Damped Additional Braces”; Fig. 4b); the insertion of both additional diagonal braces and dampers supported by the existing K-braces (ABDKB: “Additional Braces and Damped K-Braces”; Fig. 4c).

Additional braces (for all the structures in Fig. 4) and dampers (for DAB and ABDKB structures in Fig. 4(b) and Fig. 4(c), respectively) are designed according to a simple but yet effective “proportional stiffness criterion” (see Mazza and Vulcano 2001). Thus, the elastic lateral-stiffness distribution (along the structure height) of the additional braces is assumed proportional to that of the test structure in Fig. 3 (or simply, to that of a perimeter BF in Fig. 3b). In this way the stiffness ratio for the additional diagonal braces of a generic storey ($K^*_{Ba}=K_{Ba}/K_{BF}$), calculated as the ratio of the lateral stiffness of these braces (K_{Ba}) to the lateral stiffness of a BF structure (K_{BF}), is the same at each storey.

In the case of VEDs, assumptions analogous to those seen above are made for the distribution law of both the storage stiffness K'_D (giving rise, at each storey, to the same value of the corresponding stiffness ratio: $K^*_D=K'_D/K_{BF}$) and the loss stiffness K''_D (giving rise, at each storey, to the same value of the corresponding stiffness ratio: K''_D/K_{BF}).

With regard to the FRDs, whose deformability in the absence of slippage is negligible, the distribution law of the slip-load N_{Fr} is assumed similar to that of the elastic axial force induced in the braces by the lateral loads (e.g. the static horizontal loads equivalent to the wind action) before the slippage, aiming to get that the total dissipated energy to be as large as possible. In so doing, the

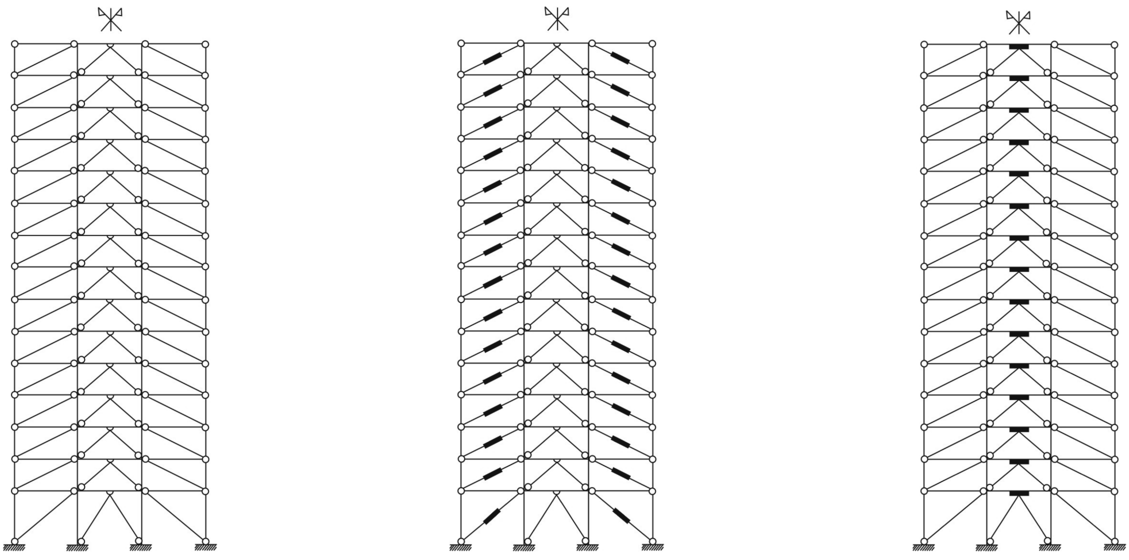

(a) (b) (c)

Fig. 4 Alternative structural solutions for controlling the along-wind response of the test structure (perimeter BF): (a) AB, “Additional Braces”; (b) DAB, “Damped Additional Braces”; (c) ABDKB, “Additional Braces and Damped K-Braces” slip-load ratio $N^*(=N_{Fr}/N_{max})$ is assumed constant at each storey, being N_{max} the axial force attained in a brace under service wind loads (e.g. the wind loads with a return period of 5 years); this axial force is assumed as an upper bound for the slip-load N_{Fr}. At last, the optimum value of N^* is selected by a criterion of minimization with reference to a parameter representative of the vibration control (Vulcano 1994), e.g., the maximum acceleration at the top storey of the building.

4. Numerical results

The dynamic analysis of the test structures in the time domain is carried out by a step-by-step procedure based on a two-parameter implicit integration scheme and an initial-stress-like iterative procedure (Casciaro 1975), already adopted by the authors for the nonlinear dynamic analysis of damped braced frames (Vulcano 2000, Mazza and Vulcano 2001). In this paper, a linearly elastic behaviour is assumed for both girders and columns, neglecting their shear deformation. An elastic-linear law, in tension and compression, is adopted for the existing and additional braces, providing for the prevention of buckling. A rather low value of the viscous damping ratio (e.g. ξ=2%) is assumed to account for damping properties of the building, except VEDs or FRDs. The response of the VEDs and the FRDs is simulated by using the models presented above (see Fig. 1 and Fig. 2, respectively). Specifically, the mechanical properties of the VE material (i.e. the laws $G'(\omega_D)$ and $G''(\omega_D)$) are assumed on the basis of the experimental data obtained by Shen and Soong (1995) for a polymeric material at an ambient temperature of 38°C; the nominal values of K'_D and K''_D (as well as the corresponding stiffness ratios) are assumed with reference to the values of G' and G'' corresponding to the fundamental frequency of the entire structural system.

For the sake of simplicity, only the along-wind component of the velocity is taken into account. The instantaneous wind velocity at each floor level of the building is given by the superposition of a mean wind velocity, with a logarithmic profile depending on the surface roughness, and a zero mean velocity fluctuation, corresponding to a stochastic stationary Gaussian process. More precisely, wind loads are schematized by means of the equivalent wind spectrum technique (Solari 1988). The equivalence criterion is formulated by defining a fictitious velocity fluctuation, which is a random function of time but invariant and perfectly cross-correlated in space. A Monte Carlo simulation is adopted to generate time histories of the wind velocity at each floor level assuming: a duration of 600 s, a step Δt=0.05 s and a return period T_r=5 years. The perception thresholds associated with various degrees of human discomfort are formulated in terms of critical values of the wind-induced building acceleration (e.g. for the sake of simplicity, according to Simiu and Scanlan 1986, assuming the maximum acceleration, a_{max}: imperceptible, for a_{max}<0.5%g; perceptible, for a_{max}=0.5%g÷1.5%g; annoying, for a_{max}=1.5%g÷5%g; etc.). Of course, this criterion is conventional because the discomfort thresholds generally depend on the frequency of motion and individual response.

At first, the effectiveness of either additional diagonal braces (AB structure) or VEDs in the DAB structure is investigated. To this aim, in Fig. 5(a) and Fig. 5(b) the maximum values attained, respectively, by the top displacement and the top acceleration, are reported against the stiffness ratio of the additional braces K^*_{Ba} (the value K^*_{Ba}=0 corresponds to the primary test structure or, simply, to the perimeter BF); moreover, the results for the DAB structure are obtained assuming the values 0.2 (relatively low) and 1.0 (relatively high) for the stiffness ratio of the VEDs, K^*_D.

With regard to the control of the top displacement (Fig. 5a), the AB structure proved more effective than the DAB structure. This kind of behaviour can be interpreted considering that the

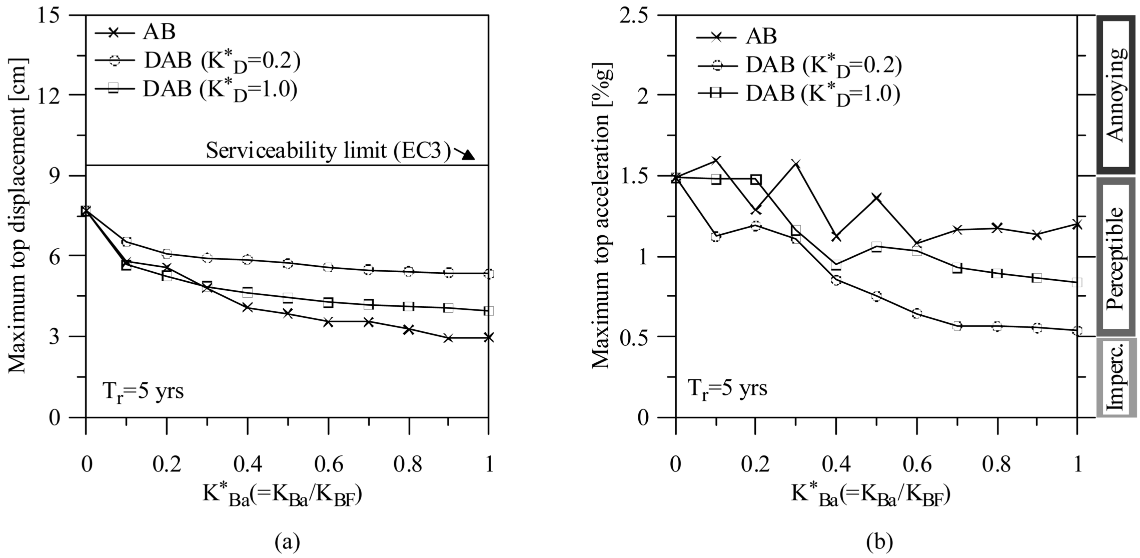

Fig. 5 Comparison of results obtained for the structures AB and DAB (with VEDs)

insertion of VEDs in series with the additional braces (as in the DAB structure) produces on the one hand an increased damping capacity, but on the other a larger deformability compared to the insertion of additional braces but no dampers (as in the AB structure). However, all the structures satisfied not only the serviceability limit imposed by EC3 on the top displacement (i.e. 1/500 of the building height, which is indicated in Fig. 5(a) by a solid line), but also the analogous limit imposed by EC3 with regard to the storey drift (i.e. 1/300 of the storey height).

With regard to the control of the top acceleration (Fig. 5b), the DAB structure (if suitably designed, e.g., assuming suitable values of K^*_{Ba}, high enough, and K^*_D, low enough) is preferable compared to the AB structure. Moreover, for a given K^*_{Ba} value, the VEDs are more effective when they are rather flexible compared to the braces supporting them (i.e. when assuming a low enough K^*_D value). Indeed, a better performance of the DAB structure for controlling the acceleration is shown by the curve corresponding to K^*_D=0.2 rather than to K^*_D=1.0, especially when a rather high value of K^*_{Ba} is assumed; however, the choice of K^*_D=1.0 is more effective in controlling the displacement (Fig. 5a).

In Figs. 6(a) and 6(b) the effects due to the insertion of both the additional braces and the VEDs on the existing K-braces of a perimeter BF are shown, comparing curves for AB and ABDKB structures. As can be observed in Fig. 6(a), the considerable increase of deformability due to the insertion of VEDs (in the ABDKB structure) is only partially balanced by the viscoelastically dissipated energy. Therefore, the additional braces should be stiff enough to keep the maximum displacement at the top floor below the limit prescribed by EC3 (e.g. with reference to the curve corresponding to K^*_D=0.2, a K^*_{Ba} value larger than 0.6 should be used). However, the effectiveness of the VEDs is evident for the control of the top acceleration (Fig. 6b), even assuming rather low values of the stiffness ratio K^*_D (e.g. equal to 0.2). A suitable choice of the K^*_D value (e.g. K^*_D=1.0), together with that of sufficiently stiff additional-braces (e.g. such that K^*_{Ba}>0.6), can lead to a maximum acceleration very close to the imperceptible threshold.

As a further confirmation of the effectiveness of the VEDs for the vibration control of DAB and

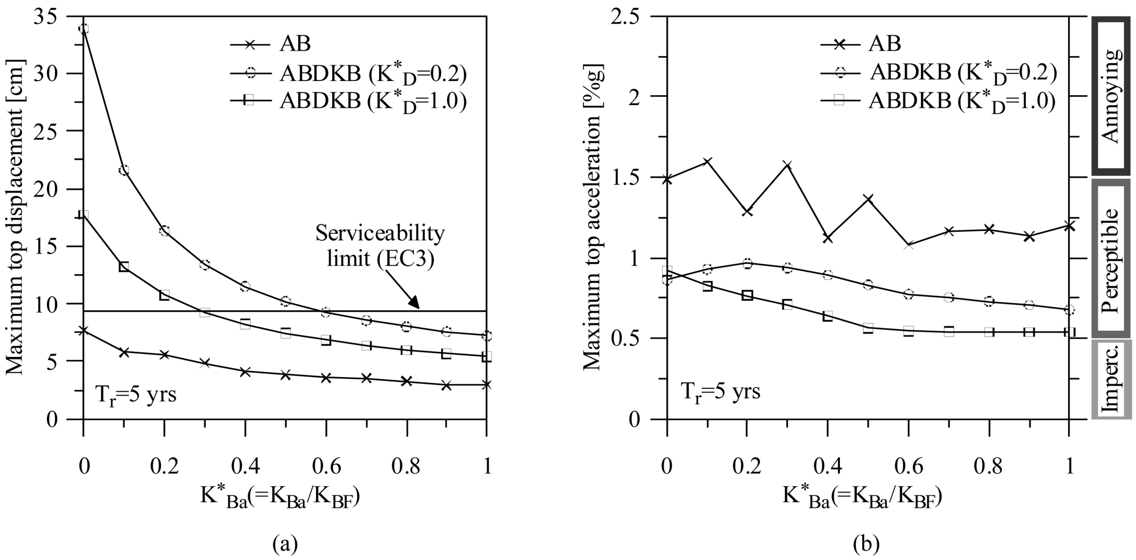

Fig. 6 Comparison of results obtained for the structures AB and ABDKB (with VEDs)

ABDKB structures, time histories of the top acceleration are plotted in Fig. 7. More precisely, the curve for the primary structure (BF) is shown in Fig. 7(a), while the curves for structures with either damped additional braces (DAB structure) or damped existing K-braces (ABDKB structure), assuming for both these structures the values K^*_D=0.2 and K^*_{Ba}=1.0, are shown in Fig. 7(b) and Fig. 7(c), respectively.

To highlight the effectiveness of additional braces and VEDs, the along-wind response at the floor levels of the primary structure (BF) is compared with the analogous response of the other structures considered in this study (AB, DAB and ABDKB). For this purpose, the maximum values attained by the floor displacement and the floor acceleration are plotted in Fig. 8(a) and Fig. 8(b), respectively. More precisely, the results were obtained assuming the same value of stiffness ratio of the additional braces (i.e. K^*_{Ba}=1.0 for AB, DAB and ABDKB structures) and, specifically for the VEDs of the DAB and ABDKB structures, a rather low value of K^*_D (i.e. K^*_D=0.2). It should be noted that, assuming K^*_{Ba}=1.0 for both the DAB and the ABDKB structures, the same value for the lateral stiffness of the braces (additional or existing, respectively) supporting the VEDs emerges, making the stiffness properties of the two structures comparable.

As shown, the DAB structure can be considered the most effective among those examined, because it ensures floor displacements quite consistent with the serviceability limit (Fig. 8a) and floor accelerations slightly exceeding the imperceptible threshold only at the top floor level (Fig. 8b).

In the following group of results attention is focused on the FRDs when inserted on a DAB structure, which, as mentioned above with reference to the VEDs, proved the most effective structural solution among those examined. To this aim, in Fig. 9(a) and Fig. 9(b) the maximum values attained at the top floor by the displacement and the acceleration, respectively, are reported for different properties of additional braces and FRDs (i.e. for different values of stiffness ratio K^*_{Ba} and slip-load ratio N^*, respectively). It should be noted that the AB structure corresponds to N^* values high enough to avoid the slippage (e.g., to $N^*\to\infty$); on the other hand, the response of the

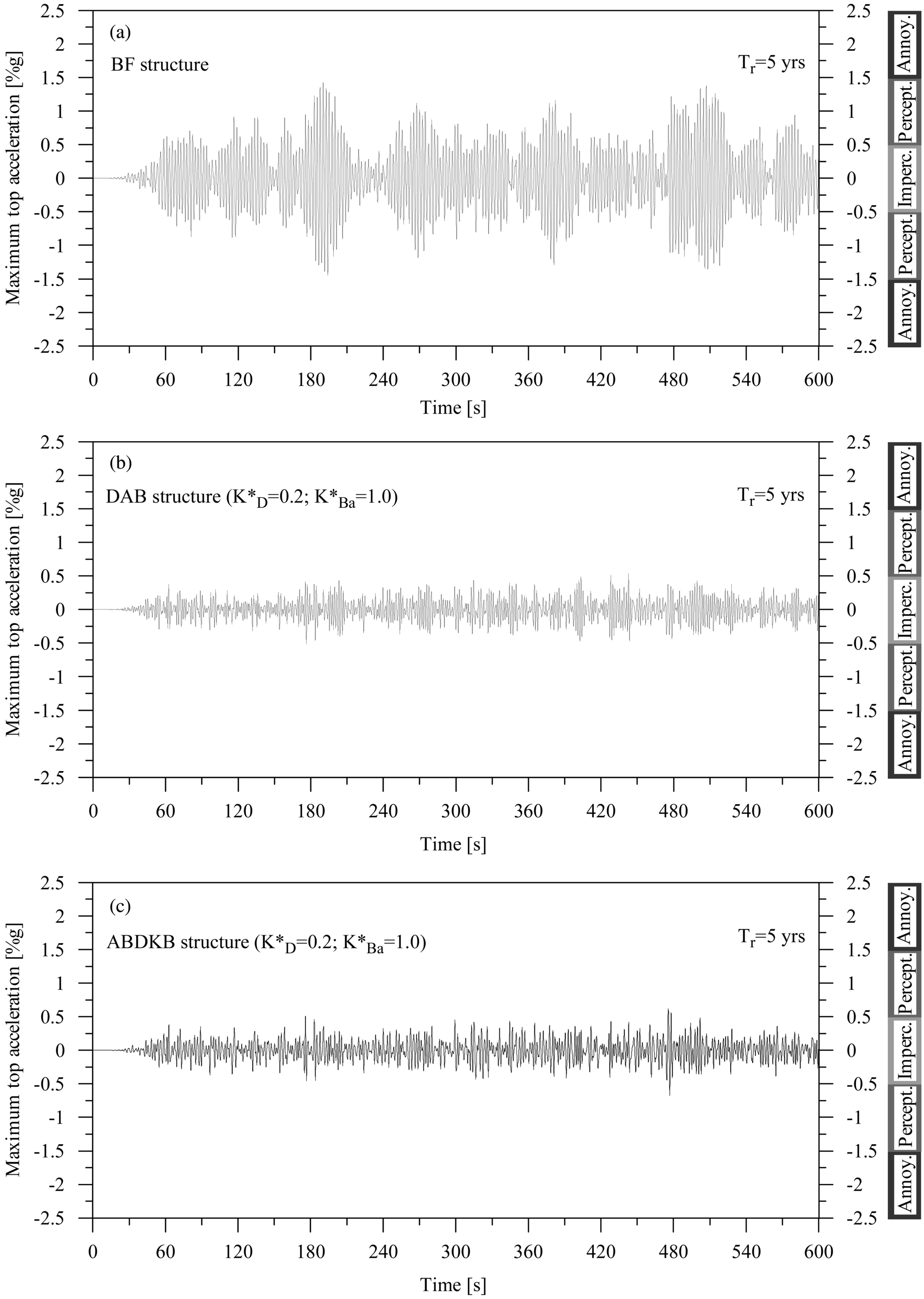

Fig. 7 Time histories of the top floor acceleration (DAB and ABDKB structures with VEDs)

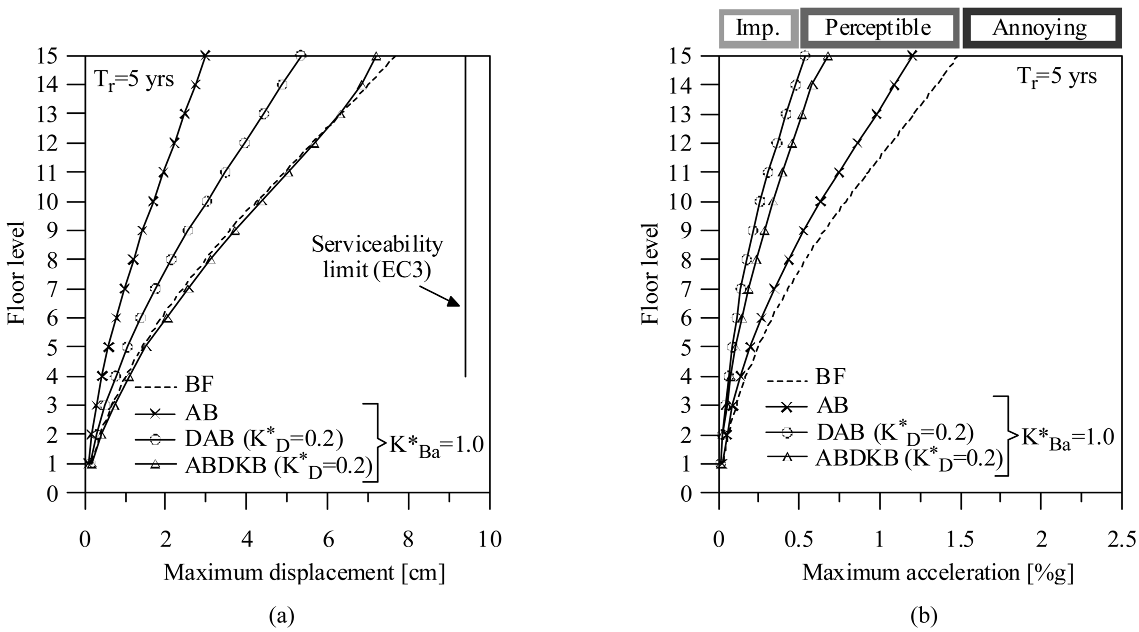

Fig. 8 Maximum values of displacement and acceleration at the floor levels (DAB and ABDKB structures with VEDs)

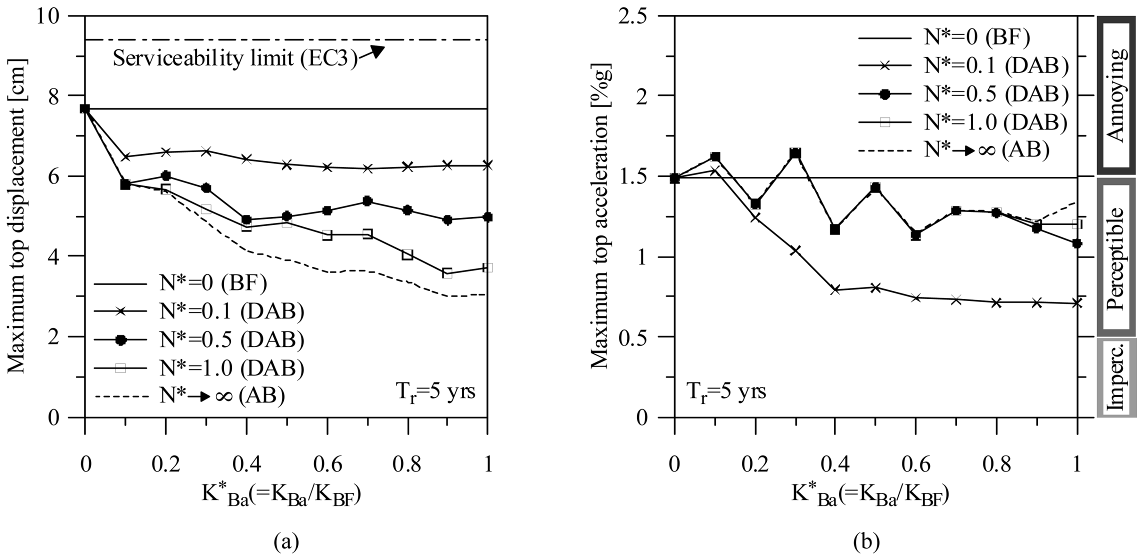

Fig. 9 Comparison of results obtained for the structures BF, AB and DAB (with FRDs)

DAB structure, for $N^{*}\to 0$, tends to that of the primary structure, BF.

As shown in Fig. 9(a), the maximum displacement, for a same value of K^{*}_{Ba}, decreases for increasing values of N^{*} (i.e., for an ever-lower expectation of slippage for the FRDs). With regard to the acceleration (Fig. 9b), the selection of the slip-load ratio N^*=0.1 corresponds to the best performance of the damped additional braces, producing, for K^*_{Ba}>0.6, only a small excess beyond the imperceptible threshold. It should be noted that the curves for N^*=0.5 or N^*=1.0 in Fig. 9(b) are very close to that for the AB structure, presenting a slight difference only for K^*_{Ba}=1.0.

The above trends are confirmed by the response in terms of maximum displacement (Fig. 10a) and maximum acceleration (Fig. 10b) at all the floor levels. More precisely, the results for the AB and DAB structures were obtained assuming the value K^*_{Ba}=1.0 for the stiffness ratio of the additional braces.

The effectiveness of either VEDs (for different values of K^*_D) or FRDs (for different values of N^*) when inserted in the DAB structure is shown in Fig. 11(a) and Fig. 11(b), respectively, representing the maximum top acceleration for different values of the stiffness ratio K^*_{Ba}. Once a K^*_{Ba} value is given, the curves in Fig. 11(a) and Fig. 11(b) allow, respectively, the optimum stiffness ratio of the VEDs ($K^*_{D,opt}$) or the optimum slip-load ratio of the FRDs (N^*_{opt}) to be selected: e.g., minimizing the maximum top acceleration corresponding to K^*_{Ba}=1.0, it can be assumed $K^*_{D,opt}$=0.1 or N^*_{opt}=0.1, respectively. It is interesting to note that VEDs and FRDs provide a comparable response when adopting these optimum values of K^*_D or N^*, respectively. However, while the selection of N^* for FRDs (Fig. 11b) should be restricted to a rather narrow range around the optimum value (N^*_{opt}=0.1), the curve referring to VEDs (Fig. 11a) shows a different shape, with a steep decrease in a range of relatively low values of K^*_D (e.g. less than 0.1) and a rather stable trend for higher values of K^*_D. This trend for the VEDs is favourable in the case when some imperfection in the calibration of the model parameters happens (e.g. when tuning the mechanical parameters G' and G'').

Lastly, the effectiveness of the VEDs and FRDs for controlling the wind response of the DAB structure is compared in Fig. 12, where the plotted curves have been obtained assuming the

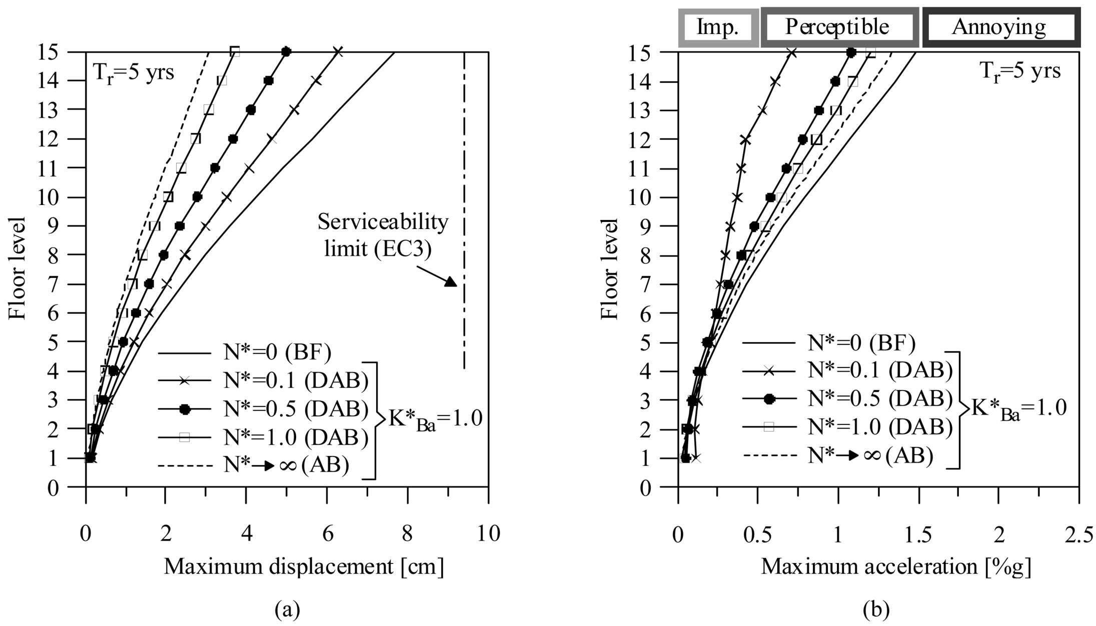

Fig. 10 Maximum values of displacement and acceleration at the floor levels of the structures BF, AB and DAB (with FRDs)

optimum value of K^*_D for VEDs (i.e. $K^*_{D,opt}$=0.1) or the analogous value of N^* for FRDs (i.e. N^*_{opt}=0.1). More precisely, the corresponding time histories of the residual energy (E_R), which is calculated as the difference between the input energy (E_I) and the energy (E_D) dissipated in viscoelasticity (i.e. by the VEDs) or Coulomb friction (i.e. by the FRDs), are compared assuming K^*_{Ba}=1.0. The results show that the shape of the E_R curves is similar for both kinds of dampers. However, the use of VEDs led generally to a lower residual energy, i.e., to a better performance compared to FRDs. Analogous results obtained for different values of K^*_{Ba}, which are omitted for

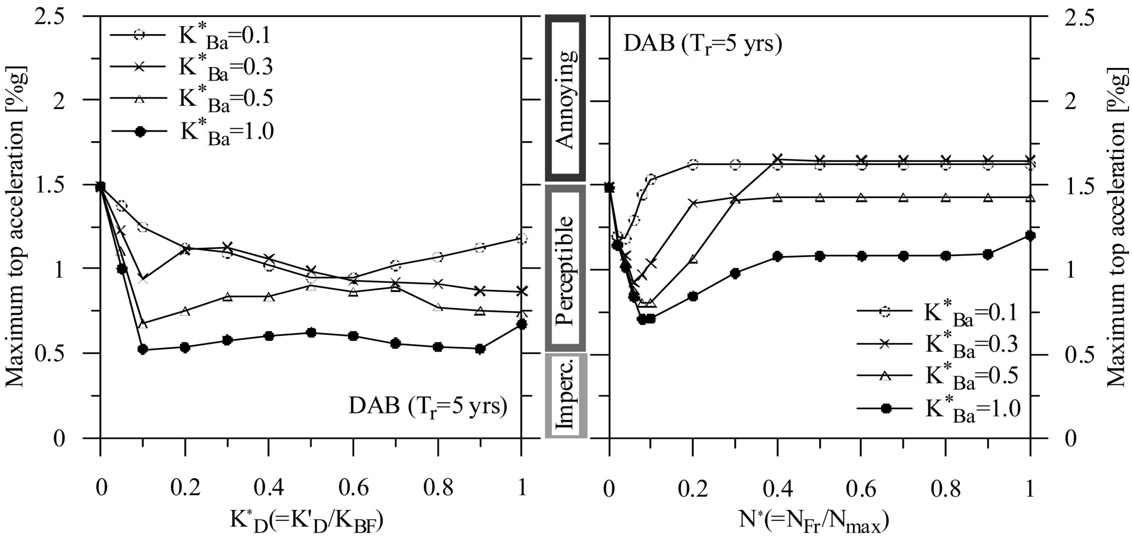

Fig. 11 Comparison of results obtained for the DAB structure: (a) with VEDs; (b) with FRDs

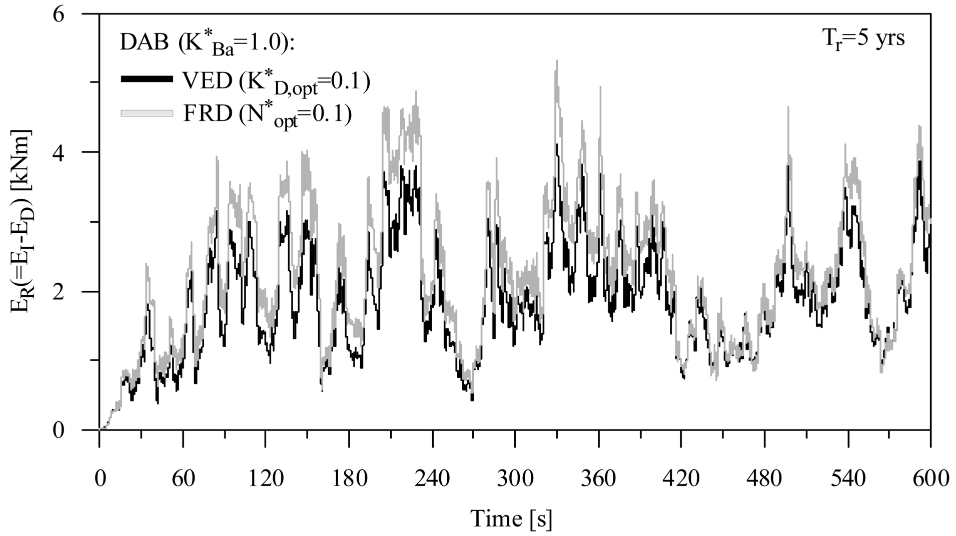

Fig. 12 Time histories of the residual energy for a DAB structure with VEDs or FRDs

the sake of brevity, proved that the better performance of the DAB structure with VEDs was more evident for an increasing value of K^*_{Ba}. Indeed, the VEDs dissipate energy also for small amplitude vibrations and, as noted above, ever-stiffer additional braces involve a better performance of VEDs with given properties.

5. Conclusions

The effectiveness of additional braces, alone or in combination with VEDs or FRDs, has been analyzed for the purpose of controlling the vibrations of a steel braced frame under wind loads with a return period T_r of 5 years. The following conclusions can be drawn from the comparison of the results obtained for the primary structure (i.e. BF) and those for alternative structural solutions derived from this structure adding braces alone (i.e. AB) or together with dampers supported by the additional braces (i.e. DAB) or the existing ones (i.e. ABDKB).

The AB structure is unsatisfactory to improve the wind response of the test structure, because it increases the lateral stiffness, so preventing large floor displacements, but, due to its low damping capacity, it is not capable of limiting the floor accelerations within a human comfort threshold.

In the cases in which VEDs are used, a DAB structure undergoes floor displacements less than the serviceability limit prescribed by EC3. However, assuming the same stiffness of the additional braces, a DAB structure proves to be less effective than the AB structure in controlling the floor displacements; the corresponding ABDKB structure (i.e. that with the same stiffness of the additional braces and properties of the VEDs analogous to those of the DAB structure) is less effective than both AB and DAB structures, involving displacements even larger than those corresponding to the primary structure, BF, unless the stiffness of the additional braces is comparable with that of the K-braces of the BF structure.

Under the same assumptions with regard to the properties of additional braces and VEDs, an ABDKB structure and, especially, a DAB one are preferable, compared to the AB structure, to control the floor accelerations, provided that the VEDs be inserted on relatively stiffer braces.

The insertion of FRDs in a DAB structure is effective in controlling the floor displacements; however, a rather low value of the slip load should be adopted in order to limit floor accelerations.

On the whole, the DAB structure proves to be, among those examined, the most effective in controlling wind-induced vibrations, particularly when using the VEDs, which, unlike the FRDs, dissipate energy also for small amplitude vibrations. In addition, the possibility of selecting a suitable value of K^*_D for the VEDs in a wide range around the optimum value is useful for a practical purpose, because the actual value of K^*_D may be different from its nominal value (e.g. due to the approximations in the calibration of the VED model).

Even though the above results were obtained for a case study, they pointed out the effects which, in general (except for super tall buildings whose vibration control is accomplished by using systems rather different from those considered above), can be induced by additional braces and (VE and friction) dampers. Indeed:

- additional braces lead, as in an AB structure, to a reduction of both displacements and accelerations, but a rather high stiffness of the braces is needed to limit the floor accelerations within the comfort threshold;
- the insertion of dampers supported by additional braces, as in a DAB structure, induces a reduction of both displacements and accelerations, because the stiffness and energy dissipation capacity of the whole is greater than those of the primary structure, but additional braces, stiffer

than those of the AB structure, are needed to limit the displacements;
- the insertion of dampers on braces of the primary structure leads, on the one hand, to an increase of the overall damping of the structure, but on the other, to a larger flexibility which may require, as in an ABDKB structure, additional braces stiff enough to limit displacements and accelerations.

References

Casciaro, R. (1975), "Time evolutional analysis of nonlinear structures", *Meccanica*, **3**, 156-167.

Eurocode 1 (2004), "Actions on structures - part 1-4: wind actions", *UNI ENV 1991-1-4.*

Eurocode 3 (2003), "Design of steel structures - part 1-1: general rules", *UNI ENV 1993-1-1.*

Housner, G. W., Bergman, L. A., Caughey, T. K., Chassiakos, A. G., Claus, R. O., Masri, S. F., Skelton, R. E., Soong, T. T., Spencer, B. F. and Yao, T. P. (1997), "Structural control: past, present and future", *J. Eng. Mech.*, ASCE, **123**(9), 897-908.

Kareem, A., Kijewski, T. and Tamura Y. (1999), "Mitigation of motions of tall buildings with specific examples of recent applications", *Wind Struct.*, **2**, 201-251.

Mazza, F. and Vulcano, A. (2001), "Modelling of viscoelastically damped braces used for the seismic protection of framed buildings", *Proc. of the 5th World Congress on Joints, Bearings and Seismic Systems for Concrete Structures*, American Concrete Institute, Rome (Italy), September.

Samali, B. and Kwok K.C.S. (1995), "The use of viscoelastic dampers in reducing wind and earthquake-induced motion of building structures", *Eng. Struct.*, **17**, 639-654.

Shen, K.L. and Soong T.T. (1995), "Modeling of viscoelastic dampers for structural applications", *J. Eng. Mech.*, ASCE, **121**, 694-701.

Simiu, E. and Scanlan, R. H. (1986), *Wind Effects on Structures*, John Wiley & Sons, New York (U.S.A).

Solari, G. (1988), "Equivalent wind spectrum technique: theory and applications", *J. Struct. Eng.*, ASCE, **113**, 1303-1323.

Soong, T. T. and Dargush, G. F. (1997), *Passive Energy Dissipation Systems in Structural Engineering*, England: John Wiley and Sons Ltd.

Tamura, Y. (1998), "Application of damping devices to suppress wind-induced responses of buildings", *J. Wind Eng. Ind. Aerodyn.*, **74-76**, 49-72.

Vulcano, A. (1994), "Design of damped steel bracing systems for seismic control of framed structures", *Proceedings of the 10th European Conference on Earthquake Engineering*, Vienna (Austria), August-September, **3**, 1567-1572.

Vulcano, A. (2000), "Use of braces with viscoelastic devices to control the vibrations of framed structures subjected to wind load" (in italian), *Proceedings of the 6th National Conference of Wind Engineering* "*IN-VENTO-2000*", Genoa (Italy), September, 381-388.

JH